SIMULATION OF A Si/SiGe MODULATION-DOPED FET USING QUANTUM HYDRODYNAMIC EQUATIONS*

J.-R. Zhou, T. Yamada, H. Miyata+, and D. K. Ferry

Center for Solid State Electronics Research
Arizona State University, Tempe, AZ 85287-6206, U.S.A.

Abstract
We present here the simulation of a Si/SiGe modulation-doped HEMT. The electron transport properties were obtained from Monte Carlo simulation. We use a set of quantum hydrodynamic equations for the device simulation. The calculated transconductance is about 300 mS/mm at 300 K. Velocity overshoot in the strained Si channel is observed. The inclusion of the quantum correction increases the total current by as much as 15 per cent.

I. Introduction

Modulation doped $Si_{1-x}Ge_x/Si/Si_{1-x}Ge_x$ offers a Si-version of the HEMT. With achievable high mobility in the strained Si layer (2000 ~ 3000 $cm^2/V\cdot s$ at 300 K [1-2], 11,000 $cm^2/V\cdot s$ at 77 K [1], and 175,000 $cm^2/V\cdot s$ at 1.5 K [3-4]), the prospects of a high performance FET are good. Experimental devices have achieved transconductance as high as 330 mS/mm at 300 K and 600 mS/mm at 77 K in a 0.25 μm gate device [1]. In this paper, we present a numerical simulation of the modulation-doped SiGe device.

In preparation for device simulation, we have obtained electron transport properties, such as the velocity-field and energy-field characteristics for strained Si and $Si_{1-x}Ge_x$ material, by Monte Carlo simulation [2]. The device modeled here has a gate length of 0.18 μm and we use a set of quantum hydrodynamic equations which utilize these Monte Carlo results. The calculated transconductance is about 300 mS/mm at 300 K. Velocity overshoot in the strained Si channel is observed. The inclusion of the quantum correction increases the total current by as much as 15 per cent.

II. Modeling of Si/SiGe modulation-doped FET

A set of hydrodynamic equations, which is described below, is used in the simulation. The equations, which are essentially the same as those used in [5-7], describe the particle conservation, momentum conservation, and energy conservation. Written in the temperature representation, we have:

$$\frac{\partial n}{\partial t} + \nabla\cdot(n\mathbf{v}) = 0, \tag{1}$$

$$\frac{\partial \mathbf{v}}{\partial t} + \mathbf{v}\cdot\nabla\mathbf{v} = -\frac{q\mathbf{E}}{m^*} - \frac{1}{nm^*}\nabla(nk_BT_q) - \frac{\mathbf{v}}{\tau_m}, \tag{2}$$

$$\frac{\partial T}{\partial t} + \frac{1}{3\gamma}\mathbf{v}\cdot\nabla(T_q) = -\frac{2}{3\gamma}\nabla\cdot(\mathbf{v}T_q) + \frac{m^*\mathbf{v}^2}{3\gamma k_B}\left(\frac{2}{\tau_m} - \frac{1}{\tau_w}\right) - \frac{T-T_0}{\tau_w}, \tag{3}$$

---

* Work supported by the Army Research Office.

+ On leave from Fujitsu Basic Processes Division, Kawasaki, Japan.

where n is the average electron density, v is the average electron velocity, T is the effective electron temperature, m^* is the effective electron mass, **E** is the electric field, τ_m is the momentum relaxation time, τ_w is the energy relaxation time, T_0 is the lattice temperature, and T_q is given by

$$T_q = \gamma T + \frac{2}{3k_B} U_q, \tag{4}$$

with

$$U_q = -\frac{\hbar^2}{8m^*} \nabla^2 \ln(n), \tag{5}$$

and γ is the degeneracy factor [7]

$$\gamma = \gamma(\mu_f / k_B T) = \frac{F_{3/2}(\mu_f / k_B T)}{F_{1/2}(\mu_f / k_B T)}, \tag{6}$$

where F_j is the Fermi-Dirac integral, and μ_f is the Fermi energy measured from the conduction band edge. The factor γ is introduced as a correction to the total average electron kinetic energy (assuming a Fermi-Dirac distribution function):

$$w = \frac{1}{2} m^* v^2 + \frac{3}{2} \gamma k_B T + U_q. \tag{7}$$

Our Monte Carlo simulation was carried out to obtain the transport properties of the SiGe materials. The computed velocity-field and energy-field relations are plotted in Figs. 1 and 2 for strained Si grown on relaxed $Si_{0.7}Ge_{0.3}$, with modulation-doped concentrations of 1.5×10^{18} cm^{-3} and 1.0×10^{14} cm^{-3} at 300 K. The velocity curves in Fig. 1 show that, due to the higher mobility of the electrons in the strained Si, electrons have higher velocity than that in SiGe material. The low-field mobility is found to be about 3000 $cm^2/V \cdot s$, and a slightly larger saturation velocity is observed. The average electron energy (Fig. 2) for strained Si rises faster at low field because of the light transverse mass and reduced intervalley scattering, but is less at high field due to impact ionization.

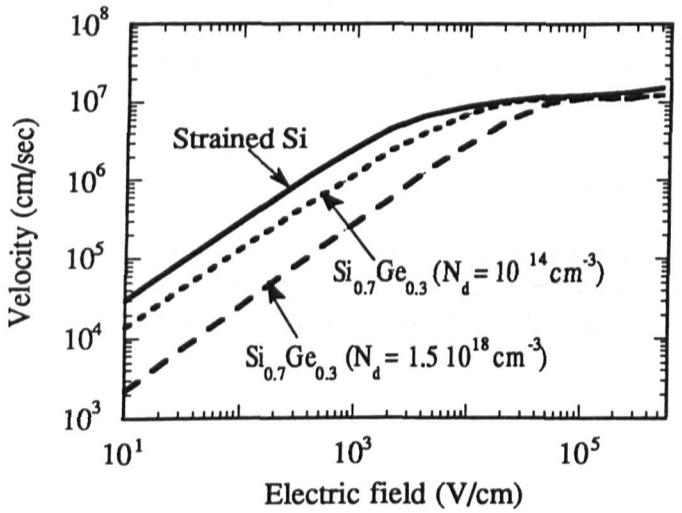

Figure 1. Velocity as a function of field for strained Si on relaxed SiGe, found from Monte Carlo simulation.

The relaxation times τ_m and τ_w, which are functions of energy, are determined by fitting the homogeneous hydrodynamic equations to the velocity-field and energy-field relations in Fig. 1 and Fig. 2.

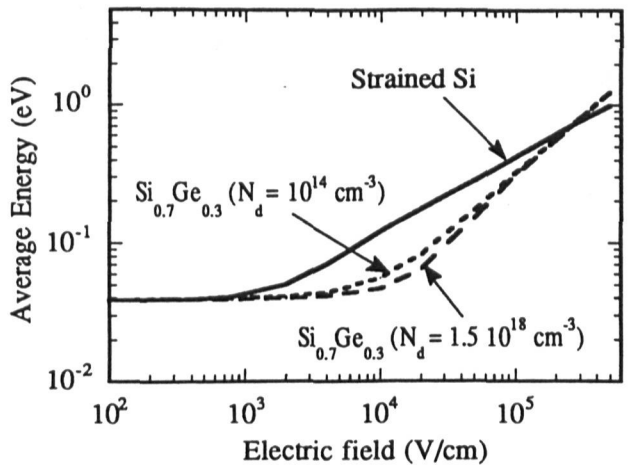

Fig. 2 Average energy as a function of field for strained Si on relaxed SiGe, found from Monte Carlo simulation.

The numerical simulation has been applied to a 0.18 μm gate, quantum-well device with a modulation-doped structure of $Si_{0.7}Ge_{0.3}/Si/Si_{0.7}Ge_{0.3}$. The device structure is shown in Fig. 3. The doping of the top $Si_{0.7}Ge_{0.3}$ layer is taken to be 3.5×10^{18} cm^{-3}, and a doping of 1.0×10^{14} cm^{-3} is used in the substrate $Si_{0.7}Ge_{0.3}$. The lattice temperature in the simulation is taken to be 300 K. The typical simulation domain is 1.0 μm × 0.095 μm. The thickness of the top SiGe layer is 19 nm, and the strained Si channel is 18 nm. The graded interface transition at the SiGe/Si junction results in an effective 3 nm spacer layer. For simplicity, we only use a three-layer structure. The modulation-doped structure in [1] is more complicated. However, the active structures are similar.

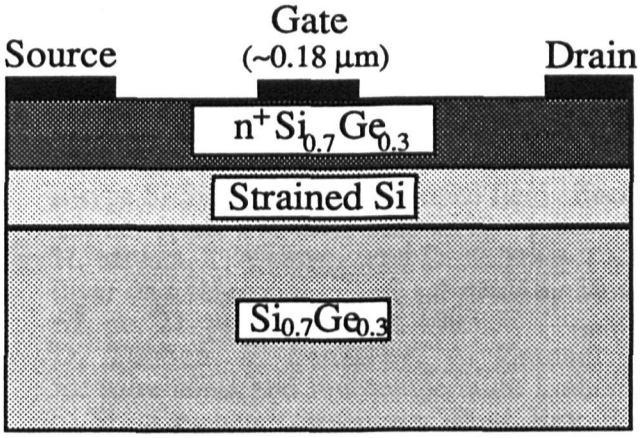

Fig. 3 The device structure.

III. The simulation results

The computed I-V characteristics for the 0.18 μm gate device are shown in Fig. 4, for gate biases of 0.7, 0.5, 0.2, and 0 volts, respectively. The small thickness of the top SiGe layer provides a normally-off device, since a Schottky barrier height of 0.9 V leads to an estimated depletion width of 18.4 nm. The peak transconductance is about 300 mS/mm, and good saturation with a drain conductance of 4.6 mS/mm at the gate voltage of 0.5 V is obtained. Approximately the

same current level and transconductance was found in a 0.25 μm device. The simulation results are comparable to the experimented results in [1]. The relatively larger current level (0.3 mA/μm) and transconductance (330 mS/mm) found in the experiment is thought to be due to a higher sheet density (2.5×10^{12} cm^{-2} [1] compared to 1×10^{12} cm^{-2} in this simulation) in the quantum well for their particular modulation-doped structure.

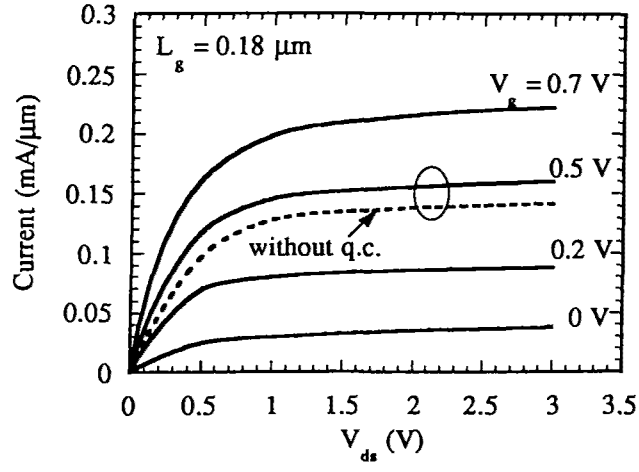

Fig. 4 I–V characteristics of a 0.18 μm SiGe device.

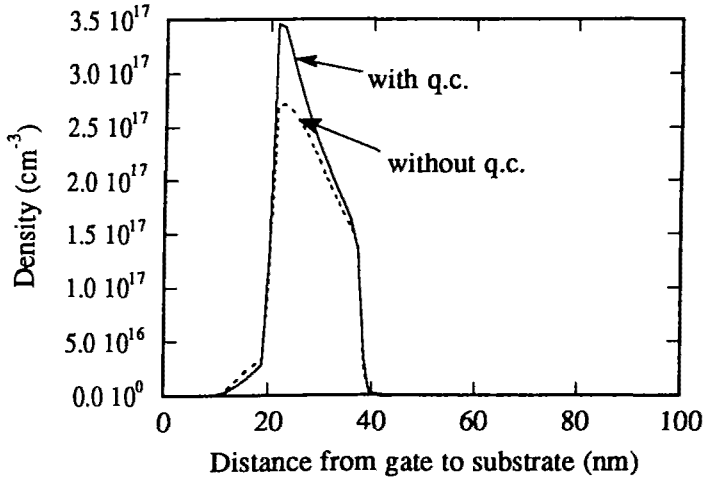

Fig. 5 Electron density across the channel.

Our simulation shows that, without including quantum corrections, the current would be 15 per cent smaller for the 0.18 μm gate device at a gate voltage of 0.5 V, as shown in Fig. 4. In other words, the inclusion of the quantum potential increases the total current by as much as 15 per cent in the simulation. This large modification of the current was not expected in the device with such a gate length. However, by inspecting the density distribution along the channel, one can find that a rapid density change occurs at the gate end close to the drain contact within a region much shorter than the gate length. In light of the quantum correction depending on the density change, the modification of the current by the quantum effects is understandable, since the electron density is high and the density change occurs in a short distance. As we expected, similar density distribution across the conduction channel (to what we found in the GaAs/AlGaAs HEMT) is found in this device [7]. The electron densities with and without quantum potential

included are plotted in Fig. 5, which shows the increase of the electron density in the channel when quantum potential is included.

Velocity overshoot, with peak velocity 2.6×10^7 cm/s, was observed in the strained Si channel for both gate lengths used in this simulation, and is very important in achieving the transconductance observed. In Fig. 6, we plot the longitudinal velocity along the conduction channel in the quantum well. The bias condition in this case is $V_g = 0.5$ V and $V_d = 1.5$ V. The velocity overshoot in the gate region results in a peak velocity of 2.6×10^7 cm/s. The overshoot is important in achieving the high transconductance for the device, for it introduces larger current flow along the quantum well. The first velocity peak in the plot is due to the model structure we used for the change of interface discontinuity [7], although it is not practical, it does suggest that the structure can increase the electron velocity between source and gate, which in turn will raise the average velocity through the device and enhance the device performance.

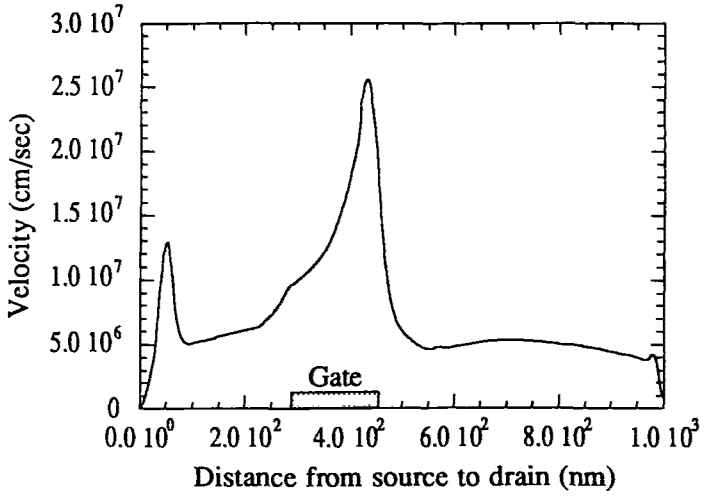

Fig. 6 Longitudinal velocity in the quantum well.

References

[1] K. Ismail, B. S. Meyerson, S. Rishton, J. Chu, and J. Nocera, "High-Transconductance n-type Si/SiGe modulation doped field effect transistors," IEEE Electron Dev. Lett. vol. 13, no. 5, pp. 229-231, May 1992 .

[2] H. Miyata, T. Yamada, and D. K. Ferry, "Electron transport properties of a strained Si layer on a relaxed $Si_{1-x}Ge_x$ substrate by Monte Carlo simulation," Appl. Phys. Lett. vol. 62, no. 21, pp. 2661-2663, 1993.

[3] D. Többen, F. Schäffler, A. Zrenner, and G. Abstreiter, "Magnetotransport measurements and low-temperature scattering times of electron gases in high-quality $Si/Si_{1-x}Ge_x$ heterostructures," Phys. Rev. B 46, pp. 4344-4347, 1992.

[4] D. Monroe, Y. H. Xie, E. A. Fitzgerald, and P. J. Silverman, "Quantized hall effects in high-electron-mobility Si/Ge structures," Phys. Rev. B 46, pp. 7935-7937, 1992.

[5] J-R. Zhou, and D. K. Ferry, "Simulation of ultra-small GaAs MESFET using quantum moment equations," IEEE Trans. Electron Devices, vol. 39, No. 3, pp. 473-478, 1992.

[6] T. J. Bordelon, X-L. Wang, C. M. Maziar, And A. F. Tasch, "Accounting for bandstructure effects in the hydrodynamic model: a first order approach for silicon device simulation," *Sol.-State Electron.*, vol. 35, no. 2, pp. 131-139, 1992.

[7] J.-R. Zhou and D. K. Ferry, " Simulation of quantum effects in ultrasmall HEMT devices," IEEE Trans. Electron Devices, vol. 40, pp. 421-427, 1993.